

Two Complementary Approaches for Weed Detection Given by Spectral and Spatial Information

J.-B. VIOIX, J.-P. DOUZALS*, J.W. LU†

F. TRUCHETET‡

L. ASSEMAT§

Abstract

The aim of this study was to detect and localize weed patches in order to improve the knowledge on weed-crop competition. A remote control aircraft provided with a camera allowed to obtain low cost and repetitive information. Different stages of image processing were necessary for the detection of weed patches. First a colorimetric base shift allows to separate the soil and plant pixels. Then, a specific algorithm including Gabor filter was able to detect crop rows on the vegetation image. Weed patches were then deduced from the comparison of vegetation and crop

* Author whom correspondence should be sent

† UMR CPAP ENESAD CEMAGREF 21, Blvd Olivier de Serres 21800 QUETIGNY, FRANCE Tel : 33 (0)3 80 77 27 48, Fax : 33 (0)3 80 77 28 16, e-mail : jb.vioix@enesad.fr, jp.douzals@enesad.fr, jw.lu@enesad.fr

‡ LE2I, IUT Le Creusot 12, rue de la Fonderie 71200 LE CREUSOT, FRANCE Tel : 33 (0)3 85 73 10 92, Fax : 33 (0)3 85 73 10 97, e-mail : f.Truchetet@iutlecreusot.u-bourgogne.fr

§ INRA, Unité de Malherbologie et Agronomie, BP 86510 21065 DIJON CEDEX, FRANCE Tel : 33 (0)3 80 69 32 82, Fax : 33 (0)3 80 69 32 62, e-mail : assemat@epoisses.inra.fr

1 images. Ground localization and geometric corrections were realized using georefer-
2 enced landmarks. Finally the development of a new acquisition device is introduced
3 and its first results for the discrimination of weeds and crops using the spectral prop-
4 erties are shown.

5 Keyword : weed detection, spatial analysis, spectral analysis, Gabor filter, neural
6 network, image processing.

7 **1 INTRODUCTION**

8 Weed detection was extensively studied as herbicide application has a relevant impact on
9 economics and environment. Developing a spraying strategy in the context of precision
10 agriculture needs to improve in-field detection of weeds. Weed detection using image
11 analysis was directed through different approaches. First experimental works were based
12 on the spectral signature of weeds and crops. Vrindts *et al.* [1] determined some specific
13 spectral bands to achieve weed identification. Statistical analysis were conducted to find
14 spectral properties of each species. In the same way Pollet *et al.* [2] developed an imaging
15 spectrograph. This device gave an image with the spatial dimension on vertical axis and
16 the spectral dimension on horizontal axis. Another experimental method was based on
17 morphological properties extracted from leaf shape using simple geometric shape factors
18 (elongation, diameter, ...)[3, 4]. In the same way Manh *et al.* used deformable tem-
19 plates to modelize leaf shape[5, 6]. In these two last cases high resolution images was
20 needed. Moreover computation time was very important and limited this application to
21 small areas. In-field detection of weeds was also possible on stubble. For example, Biller
22 *et al.* [7] achieved a sensor to detect plants on bare soil. In this case, two optical bands
23 as red (650 nm) and infra-red (850 nm) were used to find vegetation . The difference

1 between the two wavelengths was determined and controlled online spraying. Finally,
2 last approach concerned remote sensing imaging. For example aerial images taken with
3 four cameras equipped with optical band-pass filters were used by Rew *et al.* [8] to find
4 wild oat in triticale crop . They showed the increase in normalized difference vegetation
5 index (NDVI) with wild oat infestation. All these previous approaches were conducted in
6 order to discriminate weeds and crops from their spectral signature or shape. The objec-
7 tive of this paper is to develop complementary spectral and spatial methods upon aerial
8 photographs in order to improve weed detection and localization.

9 **2 ACQUISITION AND PREPROCESSING**

10 **2.1 Image acquisition**

11 A remote control aircraft was customized for this application. A Olympus μI^1 camera
12 was placed in the hold; the shot was manually triggered through the remote control. A
13 miniature video camera and an embedded high frequency (HF) emitter provided online
14 images of the flying-over area on a TV. Different flight altitudes were tested from about
15 ten meters up to few hundred meters. The resulting resolution was found to vary from
16 less than a centimeter per pixel up to some meters per pixel. After developing, films
17 were digitalized using a Canon CanoScan D660U scanner. 1702 by 1136 pixels images
18 on red, green, blue (R,G,B) channels were obtained. Theses images were then saved in
19 BMP format to avoid compression losses. Images analyzed in this paper corresponded to
20 weed/crop competition test fields located in INRA domain in Dijon (France).

¹aperture of 1 : 2.8 and focal of 35 mm

1 **2.2 Georectification**

2 In the case of high resolution images, only low altitudes flights were realized. Several
3 shots were then needed to get the whole field. Landmarks (black and white draughtboard)
4 were placed and georeferenced in the field using D-GPS coordinates (Trimble Pro XRS)
5 to locate images and also to give black and white references. A specific algorithm was
6 developped to give the transformation matrix between image coordinates and GPS coor-
7 dinates.

8 **3 IMAGE PROCESSING**

9 **3.1 Soil and plants discrimination**

10 Two methods are generally employed upon color images to solve this problem: texture
11 analysis or color discrimination. In most cases the first method is very efficient but ac-
12 curacy depends on soil roughness (due to clods, tyres and implements prints) and needs
13 high cost time algorithms. The second method is based on the color properties between
14 soil and vegetation. In this case the R,G,B color base is not adapted to find accurate col-
15 orimetric information on images acquired under natural light. Indeed, color levels depend
16 on lightness, that has to be separated from chromatic values. The HSV (hue, saturation,
17 value) color base allows this separation but RGB-HSV transformation appears to be non-
18 linear and unstable for low RGB values. Steward and Tian [9] described another color
19 base which is a linear combination of RGB values that appeared to be more adapted to
20 vegetation images.

$$\begin{bmatrix} V_1 \\ V_2 \\ I \end{bmatrix} = \begin{bmatrix} -\frac{1}{\sqrt{2}} & \frac{1}{\sqrt{2}} & 0 \\ -\frac{1}{\sqrt{6}} & \frac{1}{\sqrt{6}} & \frac{2}{\sqrt{6}} \\ \frac{1}{\sqrt{3}} & \frac{1}{\sqrt{3}} & \frac{1}{\sqrt{3}} \end{bmatrix} \cdot \begin{bmatrix} R \\ G \\ B \end{bmatrix} \quad (1)$$

1 The equation 1 describes a base rotation. The three vectors (V_1, V_2, I) are unitary and
 2 perpendicular, so information are fully independent. I corresponds to the luminosity vec-
 3 tor including shadows and other lightness defaults such as reflects.

4 (V_1, V_2) provide a colorimetric plane. V_1 is defined as the difference between red and
 5 green channels. Then V_1 is positive for vegetation pixels and negative for soil pixels. In
 6 this paper only positive values of V_1 were considered.

7 **3.2 Seed frequency characterization**

8 Previous image treatments led to vegetation images including crops and weeds. With the
 9 assumption that crops corresponded to repetitive structures, the Fourier's transform was
 10 tested. In this case each pixel was individually analyzed through his spatial distribution
 11 and V_1 intensity. The Fourier transform result corresponded to the period and the rotation
 12 angle of periodic structures. For further task, the seed frequency was characterized using
 13 a specific algorithm.

14 **3.3 Low frequencies enhancement**

15 First trials showed that the seed frequency had often a very low value generally making
 16 the filtering difficult. The size of the filter kernel depends on the frequency, a low fre-
 17 quency involves a big kernel, with inaccurate results and very long computation time. To
 18 minimize this constrain, a dilation of the lowest frequencies must be achieved. The eas-

1 iest way is an under-sampling of the image by removing a line and a column from two.
 2 This step is recursively repeated to obtain a frequency which allows an accurate filtering.
 3 In our case a value of 1/10 is needed which corresponds to about 10 pixels between two
 4 rows.

5 **3.4 Gabor filter**

6 The filter is a directive band-pass filter along the axis[10]. It was centered on ω , σ_x and
 7 σ_y set the band width respectively along the R_1 axis and the R_2 axis. Periodic structures
 8 with a frequency near ω and a rotation angle close to φ value were unchanged but other
 9 strucutres were deeply faded.

$$g(x,y) = \frac{2}{\pi\sigma_x\sigma_y} \exp\left(-\frac{R_1^2}{\sigma_x^2} - \frac{R_2^2}{\sigma_y^2}\right) \cos(2\pi\omega R_1) \quad (2)$$

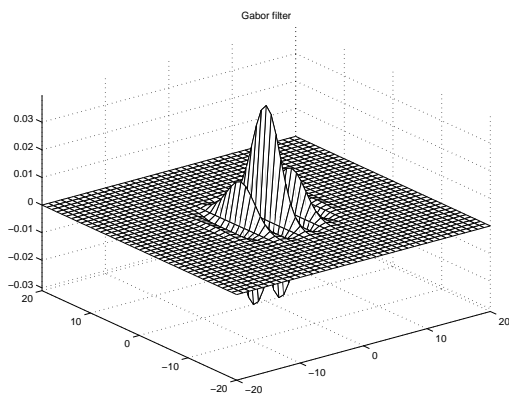
10 with

$$\begin{cases} R_1 = x \cos \varphi + y \sin \varphi \\ R_2 = -x \sin \varphi + y \cos \varphi \end{cases}$$

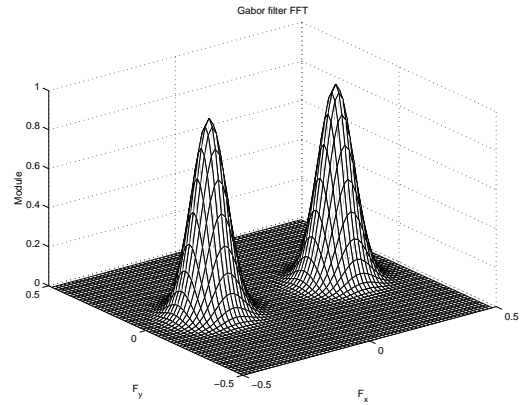
11 The spatial representation of $g(x,y)$ is shown in figure 1-a, the FFT in figure 1-b. It is a
 12 directive band pass filter centered on ω , and oriented by φ . The width is defined by σ_x and
 13 σ_y . After sampling, a mask can be defined. The size of the mask is depending on σ_x and
 14 σ_y . We truncate $g(x,y)$ on the interval $[-3\varphi, 3\varphi]$, where φ is the maximum of (σ_x, σ_y) .
 15 We keep a good approximation with an acceptable filter size.

16 **3.5 Gain computing**

17 After filtering, crops would have high value. A thresholding can be considered, but the
 18 results are not satisfying. On vector V_1 , crops and weeds have spread values. So after



(a) Spatial representation of Gabor filter



(b) Fourier transform of Gabor filter

Figure 1: Spatial and spectral representation of Gabor filter

1 filtering a low value obtained can be due to a weed pixel with high value, or a crop pixel
 2 with a low value. Then we decided to compute the gain of each pixel for an accurate
 3 thresholding (table 1). The gain is defined for each vegetation pixel as :

$$G(x,y) = \frac{p_g(x,y)}{p_{v_1}(x,y)} \quad (3)$$

4 In this equation, $p_g(x,y)$ is the module of the point after filtering, and $p_{v_1}(x,y)$ the value of
 5 this point on the vector V_1 . If the gain is near 1, the point belongs to a periodic structure
 6 defined by the coefficients of Gabor filter. For thresholding, a level of -3 dB (0.707)
 7 is generally chosen. A lowest threshold increases the band width, a higher threshold
 8 diminishes it.

Table 1: Exemple of gain computation for crop and a weed pixels

	Before filtering : p_{v_1}	After filtering : p_g	Gain : G
Crop	0.5	0.45	0.9
Weed	0.5	0.05	0.1

1 **3.6 Results**

2 We first decided to test this algorithm on synthesis images to confirm the validity of the
3 method. After this step, we tried it on images of various crops. Results depended on
4 species and vegetation stages. Crops with an important spreading out as rape and barley
5 gave bad results. Indeed the space between two rows was rapidly hidden by foliage during
6 the vegetation growth. So the discrimination was impossible with only this method. The
7 FFT did not give the seedling frequency, so the Gabor filter can not be tuned. On other
8 species the identification gave better results, and weeds can be found at early stage.

9 **3.6.1 Low altitude image**

10 The figure 2-a shows an image of a corn field (6 per 3 meters with a resolution of around
11 5 mm per pixel). Some weeds can be noticed between two rows. After the processing,
12 crops are shown in red and weeds appear in blue (figure 2-b). The end of some crop foils
13 are detected as weeds. This default is probably due to the foil shape elongation which
14 corresponds to high frequency signal.

15 **3.6.2 High altitude image**

16 Using some test field of INRA, we also aquiered high altitude images of weed patches.
17 The picture have a size was about 20 per 16 meters with a resolution close to 10 cm per
18 pixel. The crop was corn (*zea mais*) voluntary infested with green foxtail (*setaria viridis*)
19 patches at various densities. The main weed patches were well recognised, but some corn
20 foils were still detected as weeds.

1 **3.6.3 Partial conclusion**

2 The algorithm for crop row detection was efficient from a quantitative point of view.
3 Crops were well recognized, only some foil extremities were misclassified. Weeds were
4 also globally well classified. But, weeds located in crop rows were still detected as crops.
5 This result led us to complete this previous spatial analysis using a spectral approach.

6 **4 FIRST WORKS ON SPECTRAL PROPERTIES**

7 **4.1 Development of a new acquisition device**

8 Previous works have shown possibilities of spectral information for the crop/weed dis-
9 crimination [1, 11, 12]. In most studies, the visible band (red, green, blue) is completed
10 with one or several infra-red wavelengths. In the same way, we built a new acquisition
11 device based on a CCD sensor equipped with a rotating disc holding four filters. Two fil-
12 ters are band pass, one in blue (bandwidth : 50 nm , central wavelength : 500 nm) and the
13 other in the green (bandwidth : 75 nm , central wavelength : 550 nm). The two other filters
14 are high-pass at 675 nm (red) and 750 nm (infra-red) as described elsewhere ([13]). The
15 exposure time can be set at different values depending on the filter bandwidth. First trials
16 of this device were realized in laboratory with onion crops and various weeds.

17 **4.2 Crops and weeds separation using PCA**

18 Statistical tools are usually applied with multicomponent images. The principal com-
19 ponent analysis (PCA) is often used to find the base which gives the best decorrela-
20 tion between data. In our case, we can consider each pixel as a 4 component vec-

tor : $p_{i,j} = \begin{pmatrix} V_1 \\ V_2 \\ V_3 \\ V_4 \end{pmatrix}$ with i, j the coordinates of the pixel and $V_1 \cdots V_4$ the values of this

1 pixel on the four wavelengths. We can define the covariance matrix of this image as :

$$C = \frac{1}{N} \sum_{i,j} (P_{i,j} - \bar{P}) \cdot (P_{i,j} - \bar{P})^T \quad (4)$$

3 where N is the number of pixel in the image and \bar{P} the mean vector of $P_{i,j}$. The eigen-
 4 vectors of the matrix C give the base where the decorrelation is maximum. The principal
 5 component analysis was evaluated to find some difference between crops and weeds. It
 6 was computed only on the vegetation pixel to improve the discrimination. As a result
 7 some slight variations were found but these variations can not be detected by a threshold-
 8 ing. We decided to test another classifier with non-linear capabilities.

9 **4.3 Crops and weeds separation using a neural network**

10 Considering the variability of this kind of natural images, a learning classifier can be an
 11 interesting solution [14]. In this case, few pixels are classified by the operator and the
 12 system learns the principal characteristics of this train set. For first trials, a very simple
 13 neural network was developed. The input vector is the value of the pixel on the four wave-
 14 lengths. The input layer was composed of 8 cells with a linear activation function. The
 15 internal layer had the same number of neurons but with a sigmoid function which allowed
 16 a non-linear classification of data. Then, the output layer was composed of 2 neurons for
 17 weed and crop (W and C) with also a sigmoid function. The following learning rules were
 18 used. The value of 0.1 and 0.9 were preferred than respectively 0 and 1 for a better learn.

Table 2: Learning rule

	Neuron W	Neuron C
Crop	0.1	0.9
Weed	0.9	0.1
Soil	0.1	0.1

1 With these values a better convergence is obtained. So, the learning phase is faster and
 2 more accurate.

3 Two training sets were tested, both have ten pixels of crops and ten pixels of weeds,
 4 but only one set included ten pixels of soil. Only the pixels of vegetation were classified
 5 with the network. The results were slightly better when some soil pixels were considered
 6 for learning. In this case, the edge pixels were better classified. The figure 4-a shows
 7 the infra-red band of the source image. The figure 4-b and 4-c show the result of the
 8 two neurons. A simple threshold (equal to 0.5) was applied to obtain these images. The
 9 network is then able to distinguish the two classes even if there are close. For example,
 10 on the top right corner (fig 4-a) a field bindweed² leaf is covered by an onion leaf. After
 11 classification, both plants are well classified.

12 **5 CONCLUSION AND ENHANCEMENT**

13 A specific algorithm was developed in order to discriminate weed directly from an aerial
 14 photography. First results showed that weed localization was possible using spatial in-
 15 formation given after frequency analysis. The results depended on crops and vegetation
 16 stages. Nevertheless, this method appeared to be unefficient when seedlines were no more
 17 visible. Moreover, weeds located in crop rows were generally detected as crops.

18 In order to improve these previous results, species discrimination was tested through

²*Convolvus arvensis L.*

1 spectral information. A specific CCD camera was developed using four optical filters.
2 With the assumption that a correlation can be suggested between spectrometric informa-
3 tion and vegetation, various classification tools were tested. Principal component analysis
4 did not allow a classification. This was probably due to a non-linear combination of data
5 (color and specie). The neural network gave better results due to its non-linear function
6 of activation.

7 At present, the CCD camera is destined to be embedded in the drone. So, such an
8 equipment will allow to acquire spectral information at a field scale and also combina-
9 tion with spatial information. Other kind of information as image texture, shape analysis
10 would be considered. The combination of all theses information will be achieved using
11 merging tools as fuzzy logic.

12 **6 ACKNOWLEDGMENT**

13 This project is financed with the help of ITCF (French Institute for Cereal and Forage)
14 and the council of Burgundy. Authors also thank INRA (Dijon research center) for field
15 disposal.

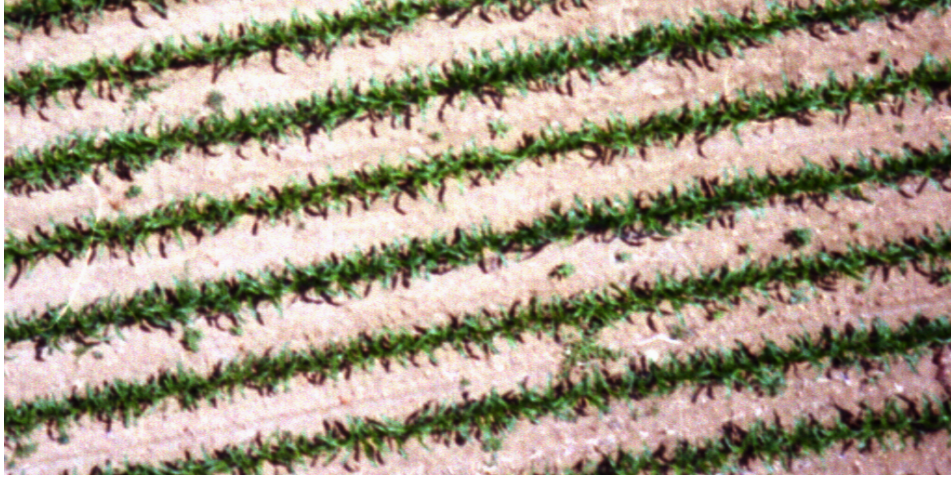
References

- [1] E. Vrindts and J. de Baerdemaeker. Optical Discrimination of Crops, Weeds and Soil for On-Line Weed Detection. In *Precision Agriculture '97*, pages 537–544. The SCI Agriculture and Environment Group, BIOS Scientific Publishers Ltd., 1997.
- [2] P. Pollet, F. Feyarts, P. Wambacq, and L. van Gool. Weed Detection Based on Structural Information Using an Imaging Spectrograph. In *Fourth International Con-*

- ference on Precision Agriculture*, pages 1537–1548. Precision Agriculture Center, ASA-CSSA-SSSA, 1999.
- [3] D. M. Woebbecke, G. E. Meyer, K. von Bargen, and D. A. Mortensen. Shape Features for Identifying Young Weeds Using Image Analysis. *Transactions of the ASAE*, 38(1):271–281, 1995.
- [4] S. Yonekawa, N. Sakai, and O. Kitani. Identification of Idealized Leaf Types Using Simple Dimensionless Shape Factors by Image Analysis. *Transactions of the ASAE*, 39(4):1525–2533, 1996.
- [5] A.-G. Manh, G. Rabatel, L. Assemat, and M.-J. Aldon. In-Field Classification of Weed Leaves by Machine Vision Using Defomable Templates. In *Third European Conference on Precision Agriculture*, pages 599–604. Agro Montpellier, 2001.
- [6] A.-G. Manh, G. Rabatel, L. Assemat, and M.-J. Aldon. Weed Leaf Image Segmentation by Deformable Templates. *J. agric. Engng. Res.*, 2001.
- [7] R. H. Biller, A. Hollstein, and C. Sommer. Precision Application of Herbicides by Use of Optoelectronics Sensor. In *Precision Agriculture '97*, pages 451–458. The SCI Agriculture and Environment Group, BIOS Scientific Publishers Ltd., 1997.
- [8] L. J. Rew, D. W. Lamb, M. M. Weedon, J. L. Lucas, R. W. Meed, and D. Lemerle. Evaluating Airborne Multispectral Imagery for Detecting Wild Oats in a Seedling Triticale Crop. In *Precision Agriculture '99*, pages 265–274. The SCI Agriculture and Environment Group, Sheffield Academic Press, 1999.

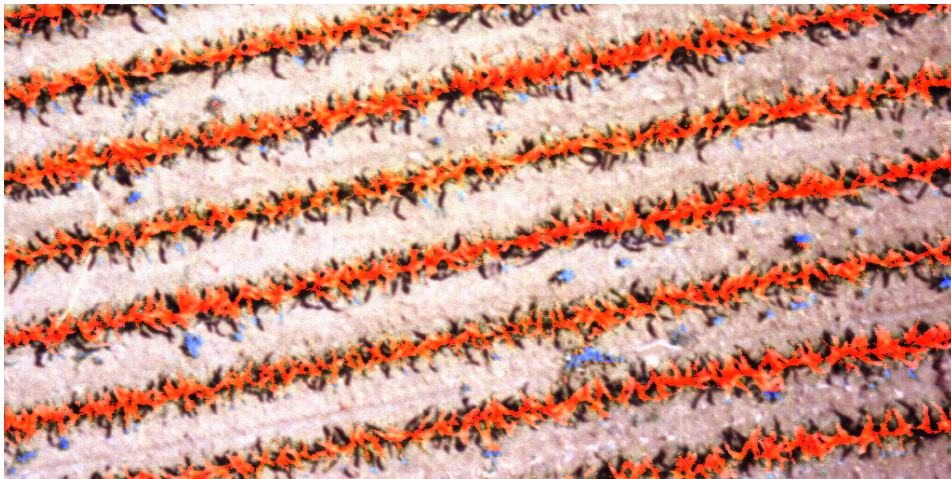
- [9] B. L. Steward and L. F. Tian. Machine-vision Weed Density Estimation for Real-time, Outdoor Lightning Conditions. *Transactions of the ASAE*, 42(6):1897–1909, 1999.
- [10] Y. Hamamoto, S. Uchimura, M. Watanabe, T. Yasuda, Y. Mitani, and S. Tomita. A Gabor Filter-Based Method For Recognizing Handwritten Numerals. *Pattern Recognition*, 31(4):395–400, 1998.
- [11] F. Feyarts, P. Pollet, L. van Gool, and P. Wambacq. Sensor for Weed Detection Based on Spectral Measurements. In *Fourth International Conference on Precision Agriculture*, pages 1537–1548. Precision Agriculture Center, ASA-CSSA-SSSA, 1999.
- [12] R. Zwiggelaar. A Review of Spectral Properties of Plants and Their Potential Use for Crop/Weed Discrimination in Row-Crops. *Crop Protection*, 17(3):189–206, 1998.
- [13] Pierre Navar. Conception et réalisation d’une caméra multispectrale. Memoire d’ingénieur, Conservatoire National des Arts et Metiers, Centre régional associé de Saône et Loire, 2001.
- [14] D. Moshou, H. Ramon, and J. de Baerdemaeker. Neural Network Based Classification of Different Weeds Species and Crops. In *Precision Agriculture ’99*, pages 275–284. The SCI Agriculture and Environment Group, Sheffield Academic Press, 1999.

Source



(a) Source image

Weeds : BLUE / Crops : RED



(b) Result image

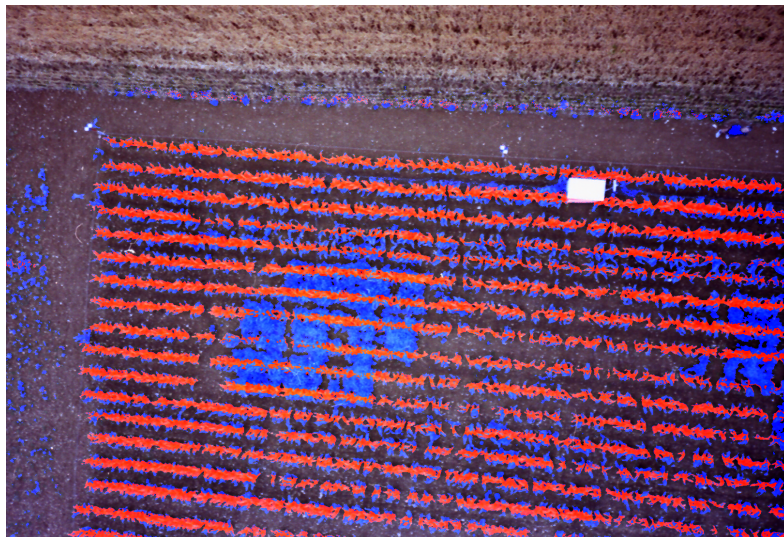
Figure 2: Source image

Source



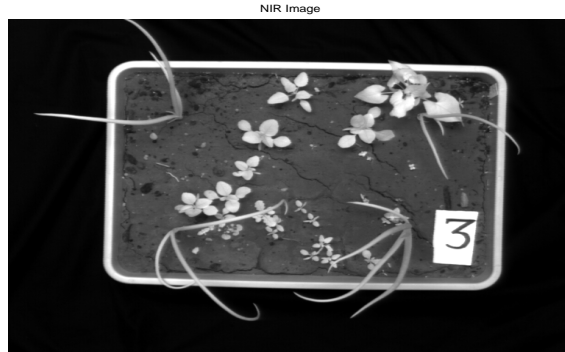
(a) Source Image

Weeds : BLUE / Crops : RED

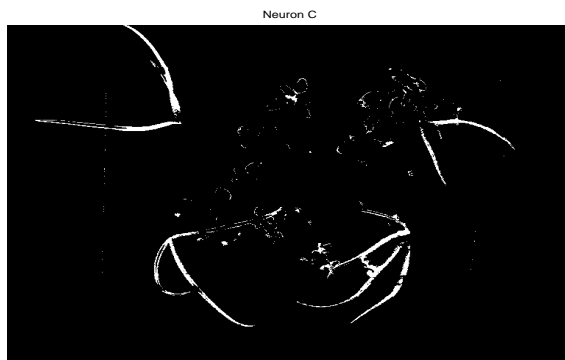


(b) Result image

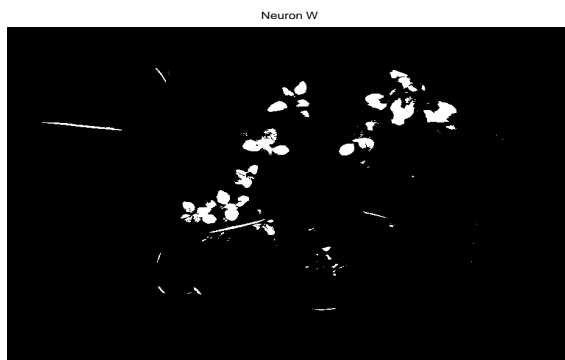
Figure 3: High altitude image



(a) Source image (IR chanel)



(b) C neuron output (Crops)



(c) W neuron output (Weeds)

Figure 4: Crop/Weed classification using a neural network